Dig Dis Sci (2014) 59:365–374
DOI 10.1007/s10620-013-2873-9

ORIGINAL ARTICLE

Characterization of Hepatocellular Carcinoma Related Genes and Metabolites in Human Nonalcoholic Fatty Liver Disease

John D. Clarke · Petr Novak · April D. Lake · Petia Shipkova · Nelly Aranibar · Donald Robertson · Paul L. Severson · Michael D. Reily · Bernard W. Futscher · Lois D. Lehman-McKeeman · Nathan J. Cherrington

Received: 18 April 2013 / Accepted: 2 September 2013 / Published online: 19 September 2013

Abstract
Background The worldwide prevalences of nonalcoholic fatty liver disease (NAFLD) and nonalcoholic steatohepatitis (NASH) are estimated to range from 30 to 40 % and 5–17 %, respectively. Hepatocellular carcinoma (HCC) is primarily caused by hepatitis B infection, but retrospective data suggest that 4–29 % of NASH cases will progress to HCC. Currently the connection between NASH and HCC is unclear.
Aims The purpose of this study was to identify changes in expression of HCC-related genes and metabolite profiles in NAFLD progression.
Methods Transcriptomic and metabolomic datasets from human liver tissue representing NAFLD progression (normal, steatosis, NASH) were utilized and compared to published data for HCC.
Results Genes involved in Wnt signaling were downregulated in NASH but have been reported to be upregulated in HCC. Extracellular matrix/angiogenesis genes were upregulated in NASH, similar to reports in HCC. Iron homeostasis is known to be perturbed in HCC and we observed downregulation of genes in this pathway. In the metabolomics analysis of hepatic NAFLD samples, several changes were opposite to what has been reported in plasma of HCC patients (lysine, phenylalanine, citrulline, creatine, creatinine, glycodeoxycholic acid, inosine, and alpha-ketoglutarate). In contrast, multiple acyl-lyso-phosphatidylcholine metabolites were downregulated in NASH livers, consistent with observations in HCC patient plasma.
Conclusions These data indicate an overlap in the pathogenesis of NAFLD and HCC where several classes of HCC related genes and metabolites are altered in NAFLD. Importantly, Wnt signaling and several metabolites are different, thus implicating these genes and metabolites as mediators in the transition from NASH to HCC.

Keywords Nonalcoholic fatty liver disease · Nonalcoholic steatohepatitis · Hepatocellular carcinoma · Metabolomics

Electronic supplementary material The online version of this article (doi:10.1007/s10620-013-2873-9) contains supplementary material, which is available to authorized users.

J. D. Clarke · A. D. Lake · P. L. Severson · B. W. Futscher · N. J. Cherrington (✉)
Department of Pharmacology and Toxicology, University of Arizona, 1703 E. Mabel Street, Tucson, AZ 85721, USA
e-mail: cherrington@pharmacy.arizona.edu

P. Novak
Southwest Environmental Health Sciences Center, College of Pharmacy, University of Arizona, Tucson, AZ, USA

P. Novak
Biology Centre ASCR, Institute of Plant Molecular Biology, Ceske Budejovice, Czech Republic

P. Shipkova · N. Aranibar · D. Robertson · M. D. Reily · L. D. Lehman-McKeeman
Bristol-Myers Squibb, Inc, Princeton, NJ, USA

Introduction

Nonalcoholic fatty liver disease (NAFLD) is a progressive liver disease that ranges from simple steatosis to the most severe form, nonalcoholic steatohepatitis (NASH). It is estimated that the prevalence of NAFLD in the adult population is between ~30 and 40 % and that up to 40 % of people with NAFLD have NASH [2]. Hepatocellular carcinoma (HCC) is the third most common cause of cancer-related death worldwide and, although hepatitis B

and hepatitis C viral infections are common risk factors [12], retrospective studies have demonstrated that cryptogenic cirrhosis is an underlying risk factor for 4–29 % of HCC cases [26, 27, 31]. Cryptogenic cirrhosis is increasingly believed to represent end stage NASH that has lost the NAFLD hallmark of steatosis [2, 28, 31] and NAFLD has been proposed as the precursor to HCC cases that arise from cryptogenic cirrhosis [6]. Although the first connection between NASH and HCC was made over two decades ago, the molecular events that link NAFLD and HCC are still not well understood. Several molecular events have been postulated to be involved in the transition from NASH to HCC including iron deposition, inflammation, oxidative stress, angiogenesis, and activation of proliferation pathways [3, 31, 32]. Along with dramatic changes in gene networks, metabolism aberrations are known to occur in HCC carcinogenesis, and several studies have identified serum biomarkers for HCC [10, 24]. Identification of differences between NASH and HCC with regard to expression of gene networks and metabolism may provide insight into the carcinogenic events that propel NASH into HCC.

Transcriptomic and metabolomic datasets from human liver samples that represent the spectrum of NAFLD, including NASH that is no longer steatotic, were utilized to determine changes that occur in Wnt signaling, extracellular matrix (ECM)/angiogenesis, and iron homeostasis gene networks. We also performed a metabolomics analysis of liver metabolites in NAFLD progression. These NAFLD-associated changes were compared to published changes that occur in HCC.

Methods

Human Liver Samples

Human liver tissue was acquired from the National Institutes of Health-funded Liver Tissue Cell Distribution System which was funded by NIH Contract #N01-DK-7-0004/HHSN267200700004C. Clinical and demographic information of these human liver samples has been described previously [13]. Tissues were collected postmortem and preserved as either frozen or paraffin embedded tissue. The samples were diagnosed as normal ($n = 19$), steatotic ($n = 10$), NASH with fatty liver ($n = 9$), and NASH without fatty liver ($n = 7$). NAFLD activity scoring categorization was done by a Liver Tissue Cell Distribution System medical pathologist [15]. Steatosis was diagnosed by >10 % fat deposition within hepatocytes without inflammation or fibrosis. NASH with fatty liver was characterized by >5 % fat deposition with accompanied inflammation and fibrosis. NASH without fatty liver was distinguished by <5 % fat deposition and increased inflammation and fibrosis. Initially, all transcript and metabolite analyses were performed using the four diagnosis categories, but due to the lack of statistical differences between the two NASH categories, these two categories were combined creating three categories: normal, steatosis and NASH.

Microarray Gene Expression Analysis

Microarray hybridization and analysis was performed in a previously published study [17]. Briefly, Affymetrix GeneChip Human 1.0 ST Arrays (Affymetrix, Santa Clara, CA, USA) were used and 33,252 genes were analyzed for differential expression between four diagnosis groups: normal, steatosis, NASH fatty, and NASH not fatty. Affymetrix® Power Tools software was employed to generate gene-level and exon-level expression signal estimates from CEL files using a multiarray mathematical algorithm. The data are publicly available at ArrayExpress public repository for microarray data under the accession number E-MEXP-3291 (http://www.webcitation.org/5zyojNu7T).

Gene Set Enrichment Analysis

A total of 283 genes that are implicated in angiogenesis and ECM processes, 85 genes implicated in iron homeostasis, and 68 genes implicated in Wnt signaling were selected using literature database searches and examination of the Kyoto Encyclopedia of Genes and Genomes (KEGG) Database (http://www.kegg.jp/). The complete list of genes is available in supplemental Table S1. For the heatmap, genes and samples were sorted using unsupervised hierarchical clustering. Clustering was performed using all genes included in the heatmap using R programming environment. Correlation was used as distance metrics and Ward's minimum variance was used as agglomeration method. These gene sets were tested for gene expression differences among the diagnosis groups using the Linear Models for Microarray Data (LIMMA) software package in Bioconductor [29]. Gene set enrichment among differentially expressed genes was tested and if they were found to have a proportion of genes that showed greater representation in up- or downregulation compared with the proportion of a randomly tested set of genes the same size, then they were considered over-represented [19]. Real-time reverse transcription-PCR was performed as previously described [21].

Western Blot

Membrane proteins (40 μg/well), cytosolic proteins (10 μg/well), or whole cell lysates (55 μg/well) were separated by SDS-PAGE and transferred to polyvinylidene difluoride membranes. A commercially available β-catenin

(Santa Cruz Biotech, Dallas, TX, USA) antibody was used. Densitometry was performed using Image Lab software (Bio-Rad Laboratories, Hercules, CA, USA). Proteins were normalized to ERK2 levels (lower ERK band) (Santa Cruz Biotech).

Immunohistochemistry (IHC)

Formal fixed paraffin embedded human liver samples were stained for localization of β-catenin using the antibody listed above. Samples were deparaffinized, rehydrated, and antigen retrieval performed (citrate buffer pH6) before endogenous peroxidase activity was blocked with hydrogen peroxide and methanol. Staining was performed using the MACH4 staining kit (Biocare Medical, Concord, CA, USA). Slides were imaged on a Leica DM4000B microscope.

Metabonomics Analytical Methods

Liver tissue samples were homogenized in ten times the tissue weight of ice-cold methanol solution with 0.1 % formic acid for 18–20 s using a polytron homogenizer over ice. Liver samples were kept frozen during all steps of the process. Samples were spun and supernatant was transferred to new tubes, gently vortexed, and each sample was added to the corresponding positions in a 96-well polypropylene plate (BrandTech Scientific, Inc. Essex, CT, USA). The 96-well plate was dried using a V&P Scientific Model VP 177 96-well plate manifold dryer (V&P Scientific Inc., San Diego, CA, USA) with nitrogen gas and processed for high resolution LC/MS analysis.

For LC/MS samples were reconstituted in a 90:10 water:methanol solution. The internal standard d_5-hippurate was added to all samples which were then injected in a randomized fashion onto a Thermo UHPLC Accela coupled to a Thermo Exactive high resolution orbitrap mass spectrometer. Ninety metabolites were acquired in positive and negative ion mode (separate injections) with a mass accuracy within 5 ppm at 25 K resolution. Metabolite area peak measurements for LC/MS quantification were calculated using Component Elucidator, a software package developed by BMS scientists.

Statistical Analysis

For microarray data, pairwise comparisons between diagnosis groups were performed using the linear models for microarray data software. A previously published method [4] was used to control the false discovery rate at the level of 0.05 to correct for multiple hypothesis testing. RT-PCR data were analyzed by one-way ANOVA with post hoc Tukey testing. LC/MS metabolomics data were analyzed by unequal variance Student's t test compared to normal. Significance (*) was determined by p values ≤ 0.05.

Results

Gene Expression Patterns Cluster According to NAFLD Diagnosis and Are Differentially Expressed in Each Gene Category

Hierarchical clustering of all 436 genes from the three gene categories revealed that the two NASH diagnoses cluster together, separate from the normal and steatosis samples (Fig. 1a). Because the two NASH categories cluster together and no statistical differences were observed between these two diagnoses, for all subsequent analyses the two categories were combined. As shown in the top left portion of the heat map (Fig. 1a), a large cluster of ECM/angiogenesis genes was upregulated in the NASH samples. An analysis of the percentage of genes with differential expression between normal and combined NASH samples was performed to assess whether genes within each category of genes were differentially expressed. In comparison to the "other" genes category, which represents all other genes in the microarray, there was a higher percentage of ECM/angiogenesis and Wnt signaling genes that were upregulated and a higher percentage of iron homeostasis and Wnt signaling genes that were downregulated (Fig. 1b). Gene set enrichment analysis confirmed that ECM/angiogenesis genes are upregulated while iron homeostasis genes are downregulated at a significantly higher rate in NASH than background genes (Table 1). We further characterized changes in the Wnt signaling pathway by dividing the Wnt pathway genes from Wnt pathway inhibitor genes and found that Wnt pathway genes showed a trend towards downregulation whereas the Wnt pathway inhibitor genes were significantly upregulated in NASH (Table 1).

Wnt Signaling Is Differentially Regulated in NASH and HCC

The expression profile of Wnt signaling genes in NASH strongly suggests inhibition of Wnt signaling. Expression of multiple Wnt frizzled receptors [*FZD3*, *FZD5*, *FZD7* (Fig. 2b)] and Wnt signaling inhibitors [*FRZB*, *SFRP5*, *DKK3*, *PRIKL1*, *PRIKL2*, *DACT1* (Fig. 2c)] are increased in NASH while the expression of Wnt ligands [*WNT3*, *WNT2* (Fig. 2b)] and Wnt activators [*FRAT1*, *PIN1* (Fig. 2d)] are decreased in NASH. Multiple

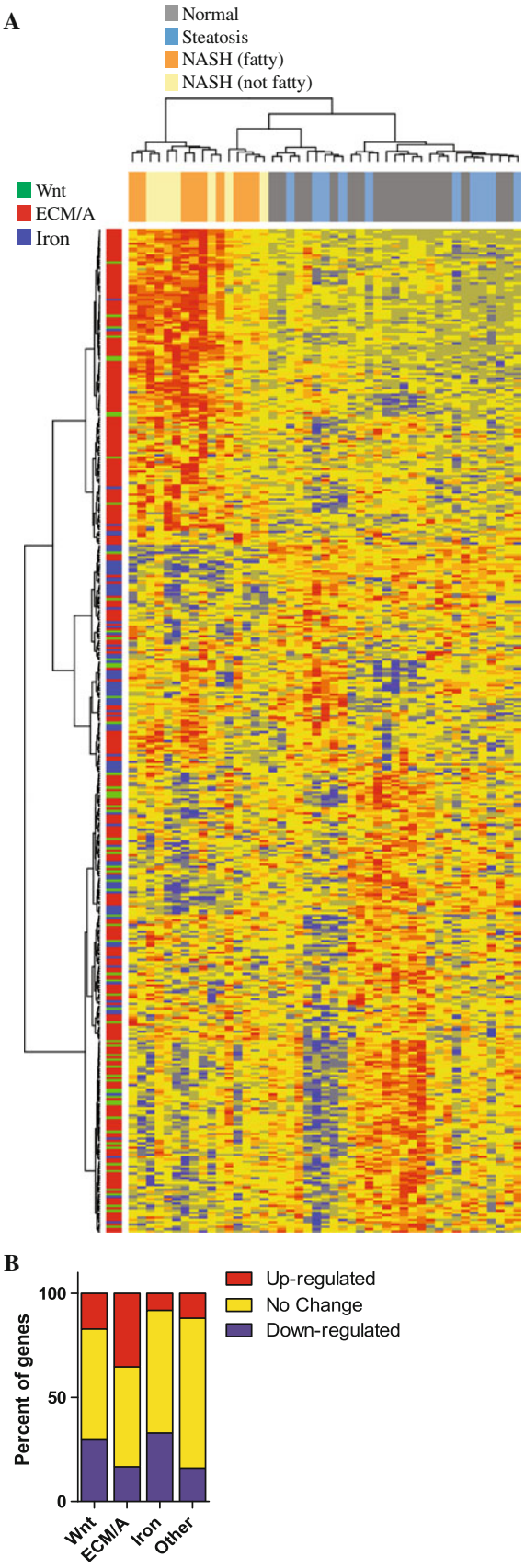

◀ **Fig. 1** Expression changes for Wnt signaling, extracellular matrix/angiogenesis (ECM/A), and iron homeostasis genes in nonalcoholic fatty liver disease (NAFLD) progression. **a** Heat map showing clustering of human liver tissues along the *top* and clustering of gene category along the *left*. Heat map colors: *red* upregulated, *blue* downregulated, *yellow* no change. **b** Percentage of genes upregulated, downregulated or not changed in a comparison of normal to NASH samples for each gene category. The "other" gene set contains all other genes from the array

Table 1 Gene set enrichment analysis of extracellular matrix/angiogenesis (ECM/A), iron homeostasis, and Wnt signaling genes in normal versus nonalcoholic steatohepatitis (NASH) liver samples

Name	Upreg. *p* value	Downreg. *p* value	*N*[a]
ECM/angiogenesis	4.84e−10	1.00	283
Iron homeostasis	0.981	0.019	85
Wnt pathway genes	0.856	0.144	53
Wnt pathway inhibitors	0.037	0.963	15

[a] Number of genes in set

downstream Wnt target genes (*CCND1*, *MYC*, *LGR5*, *GLUL*, *REG3A*, *MERTK*, *TBX3*, *EPHB2*) [5, 7, 8, 16, 38] that are known to be induced by active Wnt signaling were not changed in NASH (Fig. 2e). KEGG pathway analysis of the entire microarray dataset also suggests that Wnt signaling may be inhibited in NASH (Table 2). Western blot analysis of whole cell lysates, membrane fractions, and cytosol fractions show no change in the protein levels of β-catenin in NAFLD progression (Fig. 3a). IHC staining of β-catenin was performed to further examine its cellular localization and revealed predominately membrane staining with no nuclear staining (Fig. 3b), indicating that β-catenin is not active and translocated to the nucleus. These findings in NASH are in direct contrast to reports of active Wnt signaling in 20–90 % of HCC cases [35], downregulation of Wnt inhibitors [33, 39], and upregulation of the Wnt activator *PIN1* [23], and potentially implicate Wnt activation as a mediator in the development of HCC from NASH. The expression of selected genes from our microarray dataset was validated by qRT-PCR (compare data in Fig. 2a to corresponding gene in Fig. 2b–d).

ECM/Angiogenesis Genes Are Highly Expressed in NASH and HCC

KEGG analysis of the entire microarray dataset indicates that the ECM-receptor interactions pathway is activated in NASH (Table 2). Included within the large cluster of ECM/angiogenesis genes upregulated in NASH were five of 24 matrix metalloproteases, 14 of 23 integrin genes, seven of 12 laminin genes, and ten of 19 collagen genes (Fig. 1a). Matrix

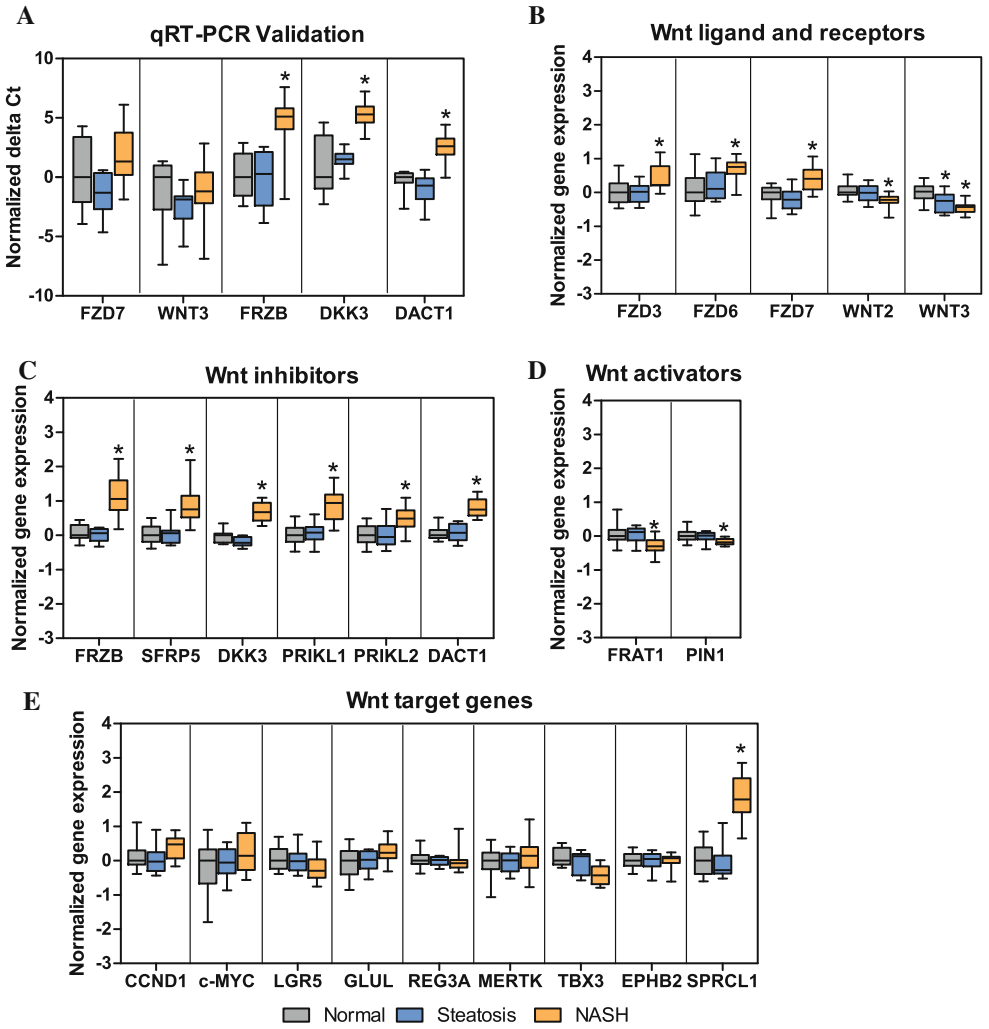

Fig. 2 Changes in Wnt signaling genes in nonalcoholic fatty liver disease (NAFLD) progression. **a** qRT-PCR validation of multiple Wnt genes. Microarray expression of Wnt ligands and receptors (**b**), Wnt inhibitors (**c**), Wnt activators (**d**), and Wnt target genes (**e**) in normal, steatosis, and nonalcoholic steatohepatitis (NASH). Data in **b**, **c**, **d** and **e**, were normalized by subtracting the median of the normal group from all other values. *Error bars* represent minimum and maximum values. Statistical significance $*p < 0.05$ compared to normal

metallopeptidase-14 (*MMP14*), integrin alpha-3 (*ITGA3*), laminin-2 (*LAMA2*), collagen type 1 alpha-2 (*COL1A2*), angiopoietin-2 (*ANGPT2*), and platelet derived growth factor receptor-alpha (*PDGFRA*) were strongly upregulated in NASH (Fig. 4a). These genes have been reported to be upregulated in HCC [18, 37]. Therefore, these changes occur early in progression to NASH and do not represent a unique event in the transition from NASH to HCC.

Iron Homeostasis Is Dysregulated in NASH and HCC

Downregulation of the master regulator of iron homeostasis, hepcidin antimicrobial peptide (*HAMP*), occurred in NASH (Fig. 4b). Iron transporters solute carrier family 11 (proton-coupled divalent metal ion transporters), member 2 (*SLC11A2*) (commonly called *DMT1*), and solute carrier family 39 (zinc transporter), member 14 (*SLC39A14*), (commonly called *ZIP14*) are both downregulated, whereas solute carrier family 40 (iron-regulated transporter), member

Table 2 Kyoto Encyclopedia of Genes and Genomes (KEGG) pathway analysis in nonalcoholic steatohepatitis (NASH)

Name	pSize[a]	NDE[b]	*p* value[c]	Status[s]
ECM-receptor interaction	84	50	5.3e−08	Activated
Pathways in cancer	326	158	6.1e−06	Activated
Wnt signaling pathway	150	58	4.9e−01	Inhibited

[a] pSize is the number of genes on the pathway

[b] NDE is the number of differentially expressed genes per pathway

[c] Bonferroni adjusted global *p* value

[d] Status indicates the direction in which the pathway is perturbed (activated or inhibited)

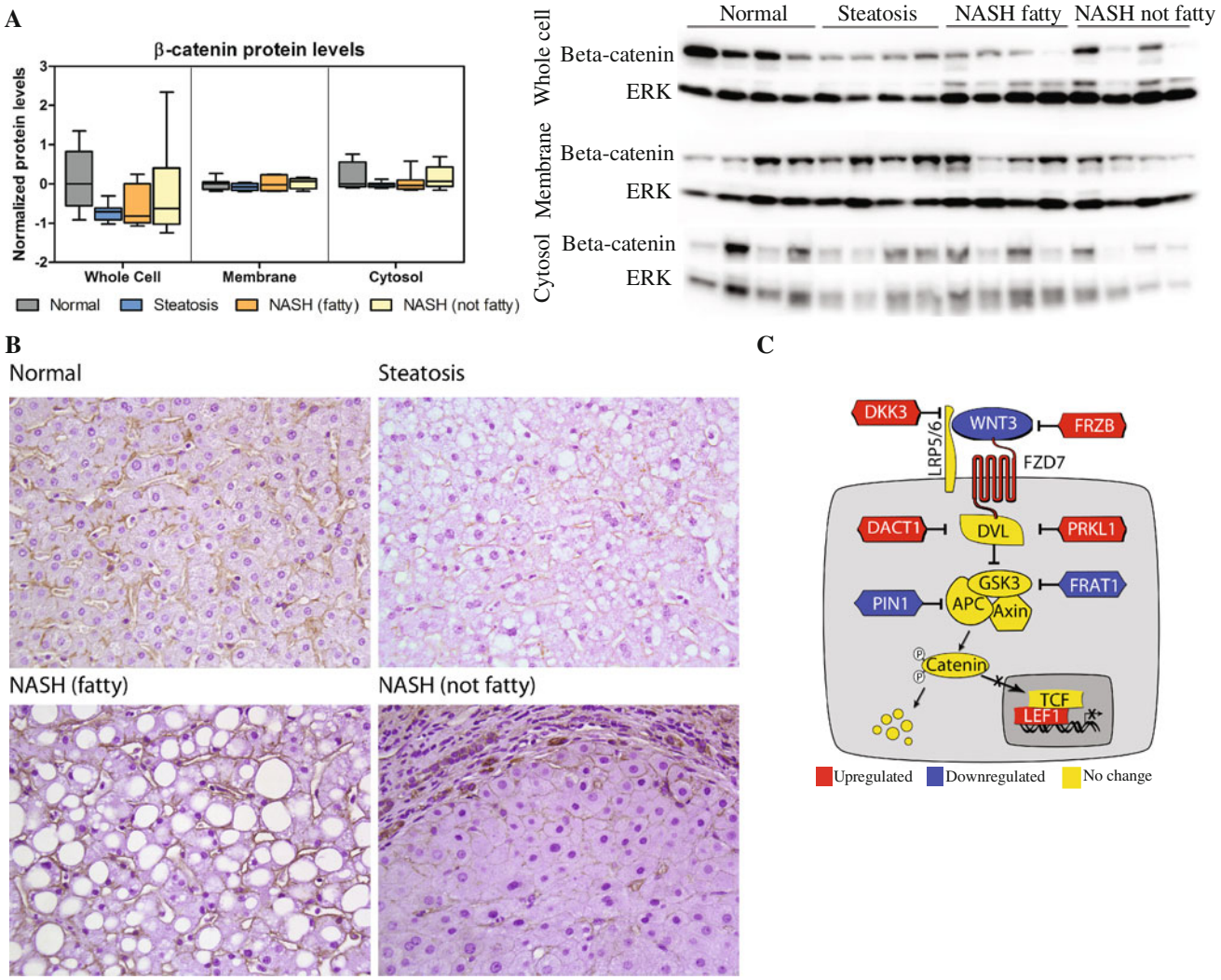

Fig. 3 β-catenin protein levels and localization in nonalcoholic fatty liver disease (NAFLD) progression. **a** Western blot of β-catenin from whole cell lysates, membrane fractions, and cytosol fractions. β-catenin protein was divided by total ERK and normalized by subtracting the median of the normal group from all other values. *Error bars* represent minimum and maximum values. **b** IHC staining of β-catenin protein localization in paraffin embedded human liver samples. **c** Representation of Wnt signaling inhibition in nonalcoholic steatohepatitis (NASH). Wnt pathway inhibitors *DKK3*, *FRZB*, *DACT1* and *PRKL1* are upregulated while Wnt pathway activators *PIN1* and *FRAT1* are downregulated in NASH progression. Multiple intermediaries and β-catenin are not changed in NASH progression

1 (*SLC40A1*) (commonly called ferroportin1), is not changed in NASH (Fig. 4c). Ferroreductases [*STEAP3* and cytochrome b reductase 1 (*CYBRD1*)] and ferroxidases [hephaestin (*HEPH*)] enzymes are dysregulated in NASH, while the ferroxidase ceruloplasmin (*CP*) was not changed (Fig. 4d). These data confirm that perturbed iron homeostasis occurs in NASH but cannot elucidate specific mechanisms that may contribute to the development of HCC.

Similarities and Differences Between Metabolite Profiles in NASH Livers and HCC Patients

To assess how changes in liver metabolite profiles in NAFLD progression compare to potential serum biomarkers for HCC, results from two recent HCC biomarker publications [10, 24] were compared to our metabolomics dataset (Table 3). A comparison of normal to steatosis samples revealed no significant changes in the metabolites presented here (data not shown). Multiple lysophosphatidylcholine metabolites were decreased in NASH, similar to reports in HCC [10, 24]. Multiple other metabolites have been reported to be decreased in plasma of HCC patients but we observed that they were increased in NASH (lysine, phenylalanine, citrulline, and creatinine) [10]. Several other metabolites that have been reported to be increased in plasma of HCC patients were decreased in NASH (glycodeoxycholic acid, creatine, inosine, and alpha-ketoglutarate) [10, 24].

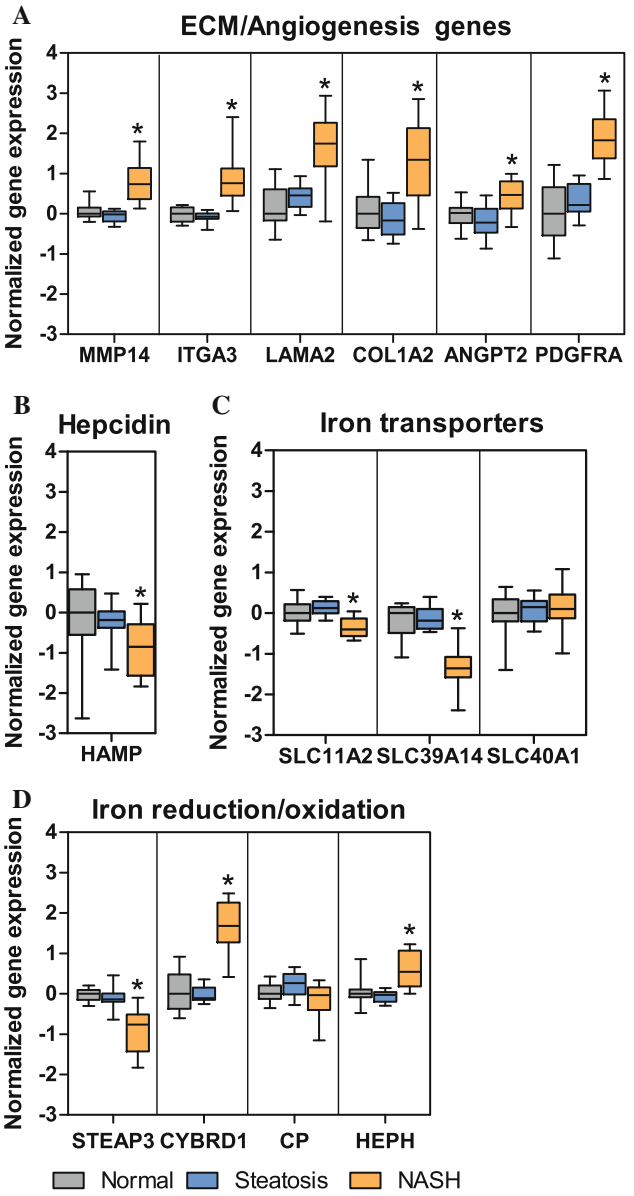

Fig. 4 Changes in extracellular matrix/angiogenesis (ECM/A) and iron homeostasis genes in nonalcoholic fatty liver disease (NAFLD) progression. **a** Microarray expression of ECM/angiogenesis genes. Iron homeostasis genes (**b**) hepcidin, (**c**) iron transporters, and (**d**) iron reduction and oxidation enzymes in normal, steatosis, and nonalcoholic steatohepatitis (NASH). Data were normalized by subtracting the median of the normal group from all other values. *Error bars* represent minimum and maximum values. Statistical significance $*p < 0.05$ compared to normal

Discussion

The present study investigated the molecular events that potentially contribute to the carcinogenesis of HCC during NAFLD progression. Our dataset contains samples representing normal, steatosis, NASH with steatosis (NASH fatty), and NASH without steatosis (NASH not fatty), with the latter category likely representing cases of cryptogenic cirrhosis. We show that the majority of changes in gene expression and metabolites occur in NAFLD progression during the transition from steatosis to NASH. Importantly, we show that there is no difference between the two NASH groups with regard to gene expression and metabolite profiles. This is consistent with several previous reports indicating that most changes in gene expression occur in the transition from steatosis to NASH [17, 32, 40]. KEGG pathway analysis of "pathways in cancer," which includes many pathways such as Jak-STAT signaling, p53 signaling, cell cycle, and apoptosis, indicates activation of cancer pathways during NAFLD progression (Table 2). This strongly suggests that the transition from steatosis to NASH initiates the process of HCC carcinogenesis, whereas loss of steatosis in NASH (i.e. progression to cryptogenic cirrhosis) does not play an important role in development of HCC. These results are consistent with a previously published microarray experiment in steatohepatitis patients [32]. In order to investigate players in the transition from NASH to HCC we identified molecular pathways that are known to be altered in HCC and

Table 3 Comparison of changes in liver metabolites that occur in nonalcoholic steatohepatitis (NASH) to changes in plasma metabolites reported to occur in hepatocellular carcinoma (HCC)

Changes	NASH	HCC	
	% of normal[a]	>1 = up <1 = down[b]	Up/down[c]
Changes in same direction			
Glycochenodeoxycholic acid	197 (↑)	6.67 (↑)	–
Taurocholic acid	298 (↑)	25.36 (↑)	–
Taurine	304 (↑)	1.45 (↑)	–
Arachidonic acid	36 (↓)	0.84 (↓)	–
Tryptophan	22 (↓)	0.76 (↓)	–
Arachidonoyl-lyso-PC (20:4)	66 (↓)	–	Down (↓)
Arachidoyl-lyso-PC (20:3)	54 (↓)	–	Down (↓)
Docosahexaenoyl-lyso-PC (22:6)	27 (↓)	0.82 (↓)	–
Linolenoyl-lyso-PC (18:2)	43 (↓)	–	Down (↓)
Linoleoyl-lyso-PC (18:3)	42 (↓)	–	Down (↓)
Palmitoyl-lyso PC (16:0)	50 (↓)	–	Down (↓)
Changes in opposite direction			
Lysine	156 (↑)	0.79 (↓)	–
Phenylalanine	158 (↑)	0.85 (↓)	–
Citrulline	297 (↑)	0.87 (↓)	–
Creatinine	255 (↑)	0.77 (↓)	–
Glycodeoxycholic acid	9 (↓)	–	Up (↑)
Creatine	53 (↓)	1.36 (↑)	–
Inosine	53 (↓)	40.62 (↑)	–
Ketoglutarate	64 (↓)	1.11 (↑)	–

Arrows in parentheses indicate direction of change in disease

[a] Percent change in metabolite levels compared to normal livers. All metabolites listed were significantly different than normal livers by Student's *t* test

[b] Serum metabolite data [10]

[c] Plasma metabolite data [24]

determined their status in NAFLD progression. A clear shortcoming for the interpretation of the present study is the comparison of changes observed in NAFLD progression to published data for HCC carcinogenesis where the HCC has not been shown to have arisen from biopsy verified NASH. In spite of this shortcoming, this study provides novel insight into potential players involved in the pathogenesis of NAFLD and subsequent progression to HCC.

Our analysis revealed multiple gene networks and metabolites that are altered similarly in NASH and HCC, while Wnt signaling and several metabolites are altered differently. Wnt signaling is commonly activated in cancer and β-catenin activation occurs in 20–90 % of HCC cases due to mutations in β-catenin, Axin, or dysregulation of β-catenin activators and inhibitors [35]. This is in direct contrast to our finding that Wnt signaling is inhibited in progression to NASH (Fig. 3c). Interestingly, gene mutations resulting in activation of the Wnt pathway occur in only about 20 % of HCC cases and, therefore, most activation of the pathway occurs through other mechanisms [33]. There have been multiple reports showing that Wnt signaling mediators involved in initiating or blocking the pathway are altered in HCC. For example, it has been shown that *WNT3* and *FZD7* are upregulated in tumors, resulting in increased β-catenin activation [14]. In NAFLD progression we observed downregulation of the Wnt ligands *WNT2* and *WNT3*, while the frizzled receptors *FZD3*, *FZD6*, and *FZD7* are upregulated. Interestingly, *FZD7* upregulation has been postulated to be an early event in HCC carcinogenesis [20] and our data support the idea that this may be a critical early event in the transition from NASH to HCC. Secreted frizzled related proteins (SFRP) can bind Wnt proteins and prevent them from binding frizzled receptors and activating Wnt signaling. Multiple SFRP genes are epigenetically inactivated in HCC by promoter methylation, while ectopic expression of SFRPs restored their inhibitory function and downregulated the β-catenin responsive transcription factors TCF/LEF in liver cancer cells [33]. In contrast to silencing of SFRPs in HCC, we observed *FRZB* and *SFRP5* are dramatically upregulated in NAFLD progression. Another Wnt signaling inhibitor, *DACT1*, has been observed to be downregulated in 43 % of human HCC samples, potentially due to promoter methylation [39]. In our dataset we observed a strong upregulation of *DACT1* expression in NAFLD progression. These data indicate that epigenetic silencing of Wnt inhibitors may be an important event in the transition from NASH to HCC. Overexpression of *DKK1*, another Wnt signaling inhibitor, in M-H7402 cells downregulated expression of c-Myc and cyclin D1, and knockdown of *DKK1* increased β-catenin, c-Myc and cyclin D1 and promoted increased migration of the cells [25]. Also, Prickle1 has been reported to be under-expressed in HCC and significantly associated with overexpression of Dvl3 and β-catenin accumulation [9]. We observed that both *DKK1* and *PRICKLE1* are dramatically increased in NAFLD progression. *PIN1* is a Wnt signaling activator which has been reported to be overexpressed in more than 50 % of HCC and was associated with increased β-catenin and cyclin D1 accumulation [23]. In contrast to these results in HCC, we show that *PIN1* expression is decreased in NAFLD progression. Collectively, these data suggest that Wnt signaling is inhibited in NAFLD progression, and activation of Wnt signaling by changes in Wnt mediators may contribute to the carcinogenesis of HCC from NASH. The precise roles of Wnt signaling in NAFLD progression and the transition from NASH to HCC need to be further investigated in controlled preclinical models before broad conclusions can be drawn.

Angiogenesis and reorganization of ECM constituents are important events in HCC progression [11, 18], and we report upregulation of many angiogenesis and ECM genes in NASH. Similar to reports in HCC [18, 37], we observed upregulation of growth factors and their receptors such as platelet derived growth factor, fibroblast growth factor, and angiopoietin. Also, upregulation of multiple matrix metallopeptidase, integrin, laminin, and collagen genes was apparent in our dataset, which is consistent with observations in HCC [18, 37]. Previous reports have explored the hypothesis that angiogenesis is important in the pathophysiology of NASH [11, 40], and our data support this hypothesis. The upregulation of these angiogenesis and ECM genes occur early in NAFLD progression and, although this likely contributes to HCC carcinogenesis, it does not represent a unique molecular event in the development of HCC from NASH.

Increased hepatic iron has been reported in NASH and HCC [22], yet greater hepatic iron scores have been reported in HCC-NASH compared to HCC-free NASH controls [30], suggesting a possible carcinogenic effect of iron overload. The mechanism for increased hepatic iron has yet to be elucidated but current findings demonstrate dysregulation of several key iron homeostasis genes in NAFLD progression that may contribute to increased iron stores. The master regulator of iron homeostasis, *HAMP*, was significantly downregulated in NASH which is consistent with previous reports in HCC [34]. In contrast to our results, however, it has been reported that serum Hamp levels were higher in patients with NAFLD [36], potentially indicating that serum and liver HAMP levels may not coincide in this context. Iron transporters are critical for the proper movement and disposition of iron and we show that the iron transporters *SLC11A2* and *SLC39A14* are downregulated in NASH progression, whereas *SLC40A1* is not changed. The liver ferroxidase *CP* and ferrireductase

STEAP3 catalyze the conversion between the ferrous and ferric iron states. The balance between the two iron oxidation states is important because iron transporters require iron to be in the ferrous state whereas iron binding by transferrin requires iron to be in the ferric state. In HCC it has been reported that *CP* is downregulated in cancerous liver tissue compared to adjacent normal tissue [34], and patients with NAFLD are more likely to have iron overload if they have lower serum *CP* levels [1]. Therefore lower CP levels are associated with both HCC and NAFLD iron overload, but in our NAFLD liver samples we did not see a change in *CP* levels. In contrast, we did observe downregulation of *STEAP3* which may lead to an accumulation of ferric iron. It is interesting to note that the intestinal ferrireductase *CYBRD1* and ferroxidase *HEPH* were both upregulated in NASH livers, although it is unclear what impact this upregulation has on iron oxidation status. Although we did not identify changes in iron homeostasis that may contribute to development of HCC from NASH, the changes we observed could perturb the removal of iron from hepatocytes due to decreased conversion into the ferrous form and transport out of intracellular vesicles thereby contributing to iron overload.

Metabolomic profiling of various liver diseases is a growing area of interest in order to identify disease biomarkers and gain understanding into disease mechanisms [10, 24]. The present study demonstrated a decline in multiple lyso-phosphatidylcholine metabolites during NAFLD progression which is consistent with a report in HCC [24]. It has been proposed that the decrease in these metabolites is caused by liver cirrhosis [24], but in our study the decrease occurred in the transition from steatosis to NASH and does not reflect an event that occurs solely during cirrhosis. We identified several metabolites that are either increased or decreased in NASH but have been reported to be changed in the opposite direction in HCC (i.e. lysine, phenylalanine, citrulline, and creatinine, glycodeoxycholic acid, creatine, inosine, and alpha-ketoglutarate). Current literature is lacking regarding the significance of these metabolites in the pathogenesis of NALFD or HCC, but the metabolite differences presented here could represent perturbations in specific metabolic pathways (Kreb's cycle, urea cycle, amino acid and purine metabolism) that may contribute to the transition from NASH to HCC.

In conclusion, this study shows that pathways important in the development of cancer are also activated in NAFLD progression and that activation of Wnt signaling potentially represents a key event in the progression from NASH to HCC. Iron homeostasis and ECM/angiogenesis signaling pathways are significantly altered in NAFLD progression and, although these molecular pathways likely augment HCC carcinogenesis, they are not unique events in the transition from NASH to HCC. These results point to several metabolites and Wnt signaling mediators that can potentially be targeted in the development of HCC from NASH. As awareness of the occurrence of NAFLD-associated HCC increases and larger more robust sample sets are obtained, the results presented here will serve as groundwork for future studies investigating the potential players in development of HCC from NAFLD.

Acknowledgments We thank the National Institutes of Health-funded Liver Tissue Cell Distribution System liver tissue samples. In particular, we thank Marion Namenwirth (University of Minnesota), Melissa Thompson (Virginia Commonwealth University), and Dr. Stephen C. Strom and Kenneth Dorko (University of Pittsburgh). Support for this work was provided by the National Institute of Health Grant [DK068039], [ES006694], [HD062489]; the NIAID grant AI083927; the National Institute of Environmental Health Science Toxicology Training Grant [ES007091]; the Liver Tissue Cell Distribution System; National Institute of Health Contract [NO1-DK-7-00041-HHSN267200700004C]; and AVOZ50510513 from the Academy of Sciences of the Czech Republic.

Conflict of interest None.

References

1. Aigner E, Theurl I, Haufe H, et al. Copper availability contributes to iron perturbations in human nonalcoholic fatty liver disease. *Gastroenterology*. 2008;135:680–688.
2. Ali R, Cusi K. New diagnostic and treatment approaches in non-alcoholic fatty liver disease (NAFLD). *Ann Med*. 2009;41:265–278.
3. Baffy G, Brunt EM, Caldwell SH. Hepatocellular carcinoma in nonalcoholic fatty liver disease: an emerging menace. *J Hepatol*. 2012;56:1384–1391.
4. Benjamini Y, Hochberg Y. Controlling the false discovery rate—a practical and powerful approach to multiple testing. *J Roy Stat Soc Ser B Method*. 1995;57:289–300.
5. Boyault S, Rickman DS, de Reynies A, et al. Transcriptome classification of HCC is related to gene alterations and to new therapeutic targets. *Hepatology*. 2007;45:42–52.
6. Bugianesi E. Non-alcoholic steatohepatitis and cancer. *Clin Liver Dis*. 2007;11:191–207.
7. Cadoret A, Ovejero C, Terris B, et al. New targets of beta-catenin signaling in the liver are involved in the glutamine metabolism. *Oncogene*. 2002;21:8293–8301.
8. Cavard C, Terris B, Grimber G, et al. Overexpression of regenerating islet-derived 1 alpha and 3 alpha genes in human primary liver tumors with beta-catenin mutations. *Oncogene*. 2006;25:599–608.
9. Chan DW, Chan CY, Yam JW, Ching YP, Ng IO. Prickle-1 negatively regulates Wnt/beta-catenin pathway by promoting Dishevelled ubiquitination/degradation in liver cancer. *Gastroenterology*. 2006;131:1218–1227.
10. Chen T, Xie G, Wang X, et al. Serum and urine metabolite profiling reveals potential biomarkers of human hepatocellular carcinoma. *Mol Cell Proteomics*. 2011;10:M110.004945-1–13.
11. Coulon S, Heindryckx F, Geerts A, Van Steenkiste C, Colle I, Van Vlierberghe H. Angiogenesis in chronic liver disease and its complications. *Liver Int*. 2011;31:146–162.

12. Di Bisceglie AM, Lyra AC, Schwartz M, et al. Hepatitis C-related hepatocellular carcinoma in the United States: influence of ethnic status. *Am J Gastroenterol*. 2003;98:2060–2063.
13. Fisher CD, Lickteig AJ, Augustine LM, et al. Hepatic cytochrome P450 enzyme alterations in humans with progressive stages of nonalcoholic fatty liver disease. *Drug Metab Dispos*. 2009;37:2087–2094.
14. Kim M, Lee HC, Tsedensodnom O, et al. Functional interaction between Wnt3 and Frizzled-7 leads to activation of the Wnt/beta-catenin signaling pathway in hepatocellular carcinoma cells. *J Hepatol*. 2008;48:780–791.
15. Kleiner DE, Brunt EM, Van Natta M, et al. Design and validation of a histological scoring system for nonalcoholic fatty liver disease. *Hepatology*. 2005;41:1313–1321.
16. Lachenmayer A, Alsinet C, Savic R, et al. Wnt-pathway activation in two molecular classes of hepatocellular carcinoma and experimental modulation by Sorafenib. *Clin Cancer Res*. 2012;18:4997–5007.
17. Lake AD, Novak P, Fisher CD, et al. Analysis of global and absorption, distribution, metabolism, and elimination gene expression in the progressive stages of human nonalcoholic fatty liver disease. *Drug Metab Dispos*. 2011;39:1954–1960.
18. Leonardi GC, Candido S, Cervello M, et al. The tumor microenvironment in hepatocellular carcinoma (review). *Int J Oncol*. 2012;40:1733–1747.
19. Luo W, Friedman MS, Shedden K, Hankenson KD, Woolf PJ. GAGE: generally applicable gene set enrichment for pathway analysis. *BMC Bioinform*. 2009;10:161–162.
20. Merle P, de la Monte S, Kim M, et al. Functional consequences of frizzled-7 receptor overexpression in human hepatocellular carcinoma. *Gastroenterology*. 2004;127:1110–1122.
21. Novak P, Jensen T, Oshiro MM, Watts GS, Kim CJ, Futscher BW. Agglomerative epigenetic aberrations are a common event in human breast cancer. *Cancer Res*. 2008;68:8616–8625.
22. O'Brien J, Powell LW. Non-alcoholic fatty liver disease: is iron relevant? *Hepatol Int*. 2011;6:332–341.
23. Pang R, Yuen J, Yuen MF, et al. PIN1 overexpression and beta-catenin gene mutations are distinct oncogenic events in human hepatocellular carcinoma. *Oncogene*. 2004;23:4182–4186.
24. Patterson AD, Maurhofer O, Beyoglu D, et al. Aberrant lipid metabolism in hepatocellular carcinoma revealed by plasma metabolomics and lipid profiling. *Cancer Res*. 2011;71:6590–6600.
25. Qin X, Zhang H, Zhou X, et al. Proliferation and migration mediated by Dkk-1/Wnt/beta-catenin cascade in a model of hepatocellular carcinoma cells. *Transl Res*. 2007;150:281–294.
26. Ratziu V, Bonyhay L, Di Martino V, et al. Survival, liver failure, and hepatocellular carcinoma in obesity-related cryptogenic cirrhosis. *Hepatology*. 2002;35:1485–1493.
27. Regimbeau JM, Colombat M, Mognol P, et al. Obesity and diabetes as a risk factor for hepatocellular carcinoma. *Liver Transpl*. 2004;10:S69–S73.
28. Siegel AB, Zhu AX. Metabolic syndrome and hepatocellular carcinoma: two growing epidemics with a potential link. *Cancer*. 2009;115:5651–5661.
29. Smyth GK. *Bioinformatics and computational biology solutions using R and bioconductor, in Limma: Linear models for microarray data*. New York: Springer; 2011.
30. Sorrentino P, D'Angelo S, Ferbo U, Micheli P, Bracigliano A, Vecchione R. Liver iron excess in patients with hepatocellular carcinoma developed on non-alcoholic steato-hepatitis. *J Hepatol*. 2009;50:351–357.
31. Starley BQ, Calcagno CJ, Harrison SA. Nonalcoholic fatty liver disease and hepatocellular carcinoma: a weighty connection. *Hepatology*. 2010;51:1820–1832.
32. Starmann J, Falth M, Spindelbock W, et al. Gene expression profiling unravels cancer-related hepatic molecular signatures in steatohepatitis but not in steatosis. *PLoS One*. 2012;7:e46584.
33. Takagi H, Sasaki S, Suzuki H, et al. Frequent epigenetic inactivation of SFRP genes in hepatocellular carcinoma. *J Gastroenterol*. 2008;43:378–389.
34. Tan MG, Kumarasinghe MP, Wang SM, Ooi LL, Aw SE, Hui KM. Modulation of iron-regulatory genes in human hepatocellular carcinoma and its physiological consequences. *Exp Biol Med (Maywood)*. 2009;234:693–702.
35. Thompson MD, Monga SP. WNT/beta-catenin signaling in liver health and disease. *Hepatology*. 2007;45:1298–1305.
36. Valenti L, Swinkels DW, Burdick L, et al. Serum ferritin levels are associated with vascular damage in patients with nonalcoholic fatty liver disease. *Nutr Metab Cardiovasc Dis*. 2011;21:568–575.
37. Villanueva A, Newell P, Chiang DY, Friedman SL, Llovet JM. Genomics and signaling pathways in hepatocellular carcinoma. *Semin Liver Dis*. 2007;27:55–76.
38. Yamamoto Y, Sakamoto M, Fujii G, et al. Overexpression of orphan G-protein-coupled receptor, Gpr49, in human hepatocellular carcinomas with beta-catenin mutations. *Hepatology*. 2003;37:528–533.
39. Yau TO, Chan CY, Chan KL, et al. HDPR1, a novel inhibitor of the WNT/beta-catenin signaling, is frequently downregulated in hepatocellular carcinoma: involvement of methylation-mediated gene silencing. *Oncogene*. 2005;24:1607–1614.
40. Younossi ZM, Gorreta F, Ong JP, et al. Hepatic gene expression in patients with obesity-related non-alcoholic steatohepatitis. *Liver Int*. 2005;25:760–771.